Supporting Information (SI) Appendix:

Network of mutually repressive metastasis regulators can promote cell heterogeneity and metastatic transitions

Jiyoung Lee[a], Jinho Lee[b], Kevin S. Farquhar[b], Jieun Yun[a,d], Casey Frankenberger[a], Elena Bevilacqua[a], Kam Yeung[c], Eun-Jin Kim[e], Gábor Balázsi[b] and Marsha Rich Rosner[a]

[a]Ben May Department for Cancer Research, The University of Chicago, Chicago, IL 60637

[b]Department of Systems Biology – Unit 950, Division of Cancer Medicine, The University of Texas MD Anderson Cancer Center, Houston, TX 77054

[c]Department of Biochemistry and Cancer Biology, The University of Toledo, Toledo, OH 43606

[d]Bioevaluation Center, Korea Research Institute of Bioscience and Biotechnology, Cheongwon, 363-883, Korea

[e]School of Mathematics and Statistics, University of Sheffield, Sheffield, S3 7RH UK

Table of Contents

1. Supplementary Table S1 and Supplementary Figures S1-S7

Primer for ChIP	Sequences (5'-3')
HMOX1-Forward (F)	CAGTGCCTCCTCAGCTTCTC
HMOX1-Reverse (R)	CTCGGTGGATTGCAACATTA
RKIP1-F	AGCAGTTTGGGAGGCTGAG
RKIP1-R	GCGCCCAGCTAATTTTTGTA
RKIP2-F	CCTGCCTGTAATCCCAGCTA
RKIP2-R	GAGTGCAGTGGCGTGATCT
RKIP3-F	TCACTCAGGTGCTCTCACCA
RKIP3-R	CCTTGCTTTTCTCCTGCACT
RKIP4-F	CTCCCAAAGTGCTGGGAATA
RKIP4-R	CTTGGTTGCGTTTTGGTTTT
BACH1-1-F	GGGAATCCATGAATACCATCC
BACH1-1-R	GATTAGGGGTGCTGGGTTTT
BACH1-2-F	CGGAAGGAGTGAGTCACCTG
BACH1-2-R	GAGCCACTCACCAGAGCTGA
BACH1-3-F	TGCTTCTTCCTGGTCTTTGG
BACH1-3-R	GCCAAAGTCACCCTACTCCA

Supplementary Table S1. Sequences of primers for ChIP-qPCR.

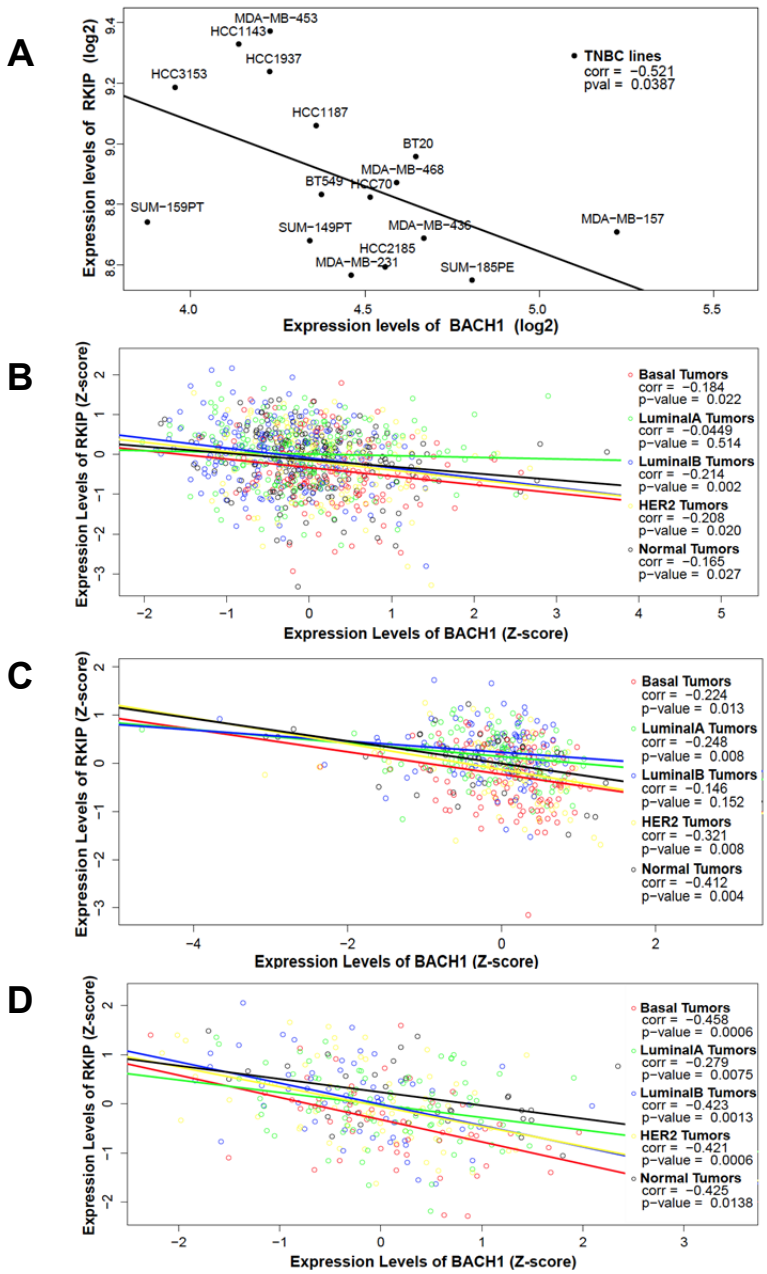

Fig.S1. BACH1 and RKIP expression in breast cancer cell lines and primary patient tumors. All analysis of correlations between mRNA expression of BACH1 and RKIP were performed in R using microarray data downloaded from the ArrayExpress, Gene Expression Omnibus (GEO) and Netherlands Cancer Institute websites. All data were preprocessed using Robust Multichip Averaging (RMA). (**A**) Expression profiles of 51 breast cancer cell lines (EtabM157, ArrayExpress) were compared using the 204194_at probe for BACH1 and 205353_s_at probe for PEBP1 (RKIP). TNBC cell lines were identified as previously described (1). Three sets of patient data were assembled from nine previously published studies; (**B**) 871 patient tumors from GEO accession numbers GSE1456, GSE2990, GSE3494, and GSE7390; (**C**) 443 patient tumors from GEO accession numbers GSE5327, GSE2034, and GSE2603; and (**D**) 295 patient tumors downloaded from the Netherlands Cancer Institute (http://bioinformatics.nki.nl/data.php). Patient data was z-score transformed after RMA processing, duplicate gene probes were filtered for the highest variance, and tumors were molecularly subtyped into basal, HER2+, luminal A, luminal B and normal-like classes as previously described (2-4). The degree and significance of correlations were calculated using Pearson's method.

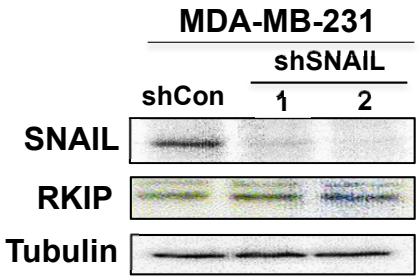

Fig.S2. SNAIL-depletion does not change RKIP levels.
MDA-MB-231 cells were stably depleted for SNAIL using shRNA as described in Materials and Methods. SNAIL and RKIP protein levels were measured by Western blotting.

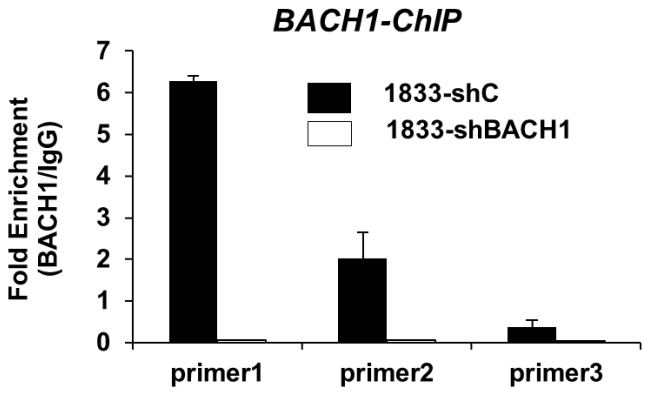

Fig.S3. BACH1 is directly recruited to the RKIP promoter.
ChIP assays represent preferential BACH1 recruitment at -8,744 bp (Primer1) in the BACH1 promoter in 1833 cells. BACH1-depleted 1833 cells were used as negative control. Error bars represents SEM value from 3 independent experiments.

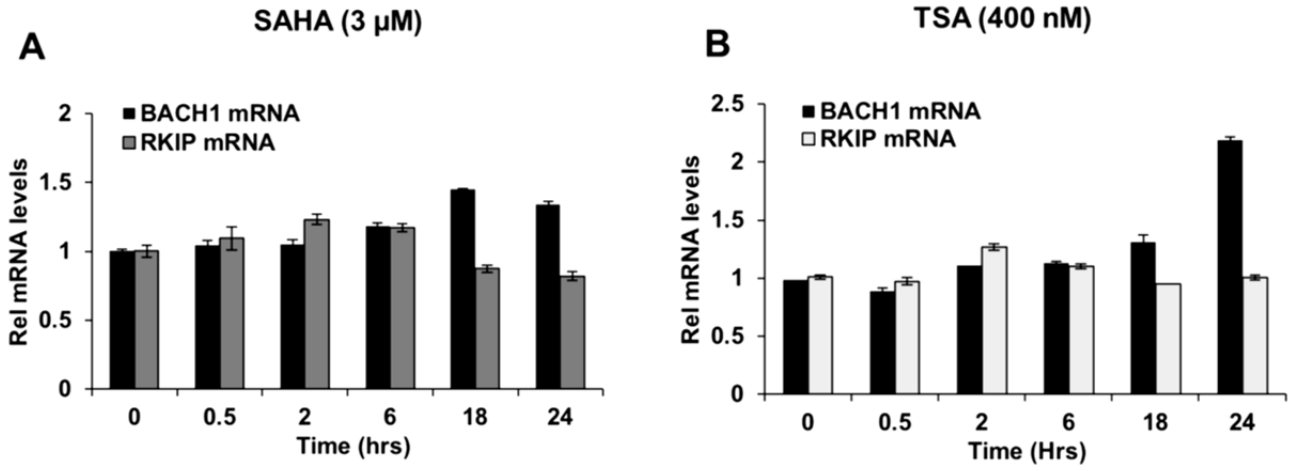

Fig. S4. HDAC inhibitors (SAHA and TSA) do not change BACH1 levels in 6 hrs.
MDA-MB-231 cells were treated with SAHA (**A**) or TSA (**B**) for 0.5, 2, 6, 18 and 24 hrs. Total RNA was prepared as described in Methods. BACH1 and RKIP mRNA levels from cells were analyzed by qRT-PCR. Error bars represent SEM value from 3 independent experiments.

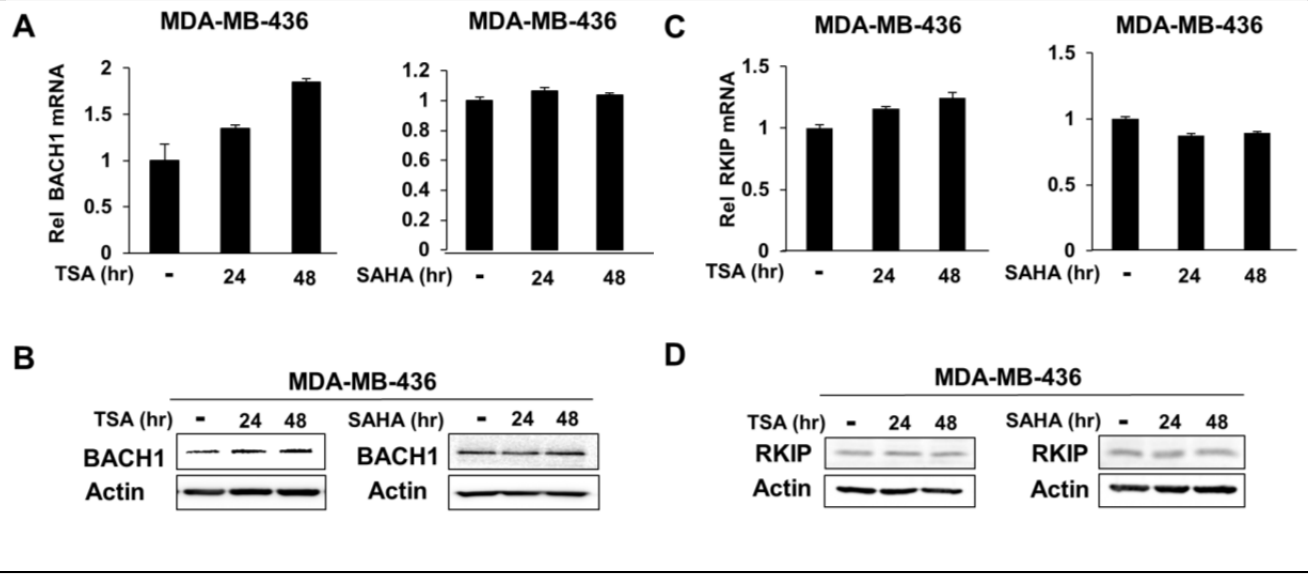

Fig. S5. BACH1 and RKIP expressions following TSA or SAHA treatment in MDA-MB-436 cells.
MDA-MB-436 cells were treated for the indicated times with TSA or SAHA as described in Materials and Methods. Quantification of mRNA and protein levels of BACH1 (**A**,**B**) and RKIP (**C**,**D**) were analyzed. Error bars represent SEM value from 3 independent experiments.

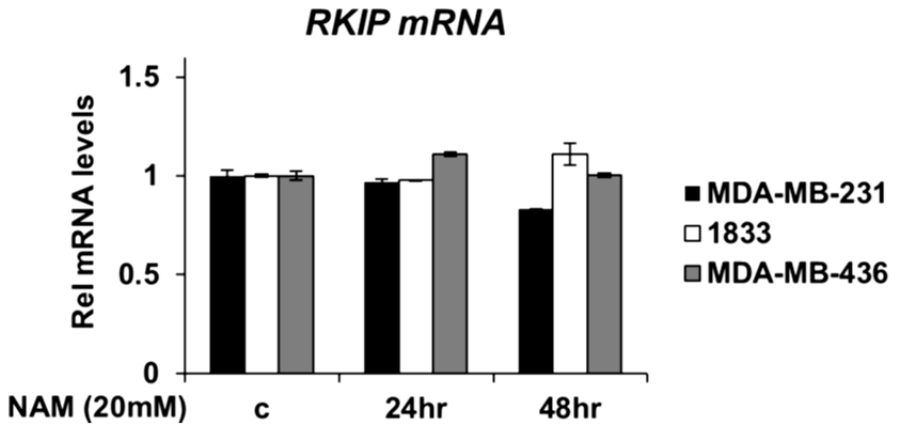

Fig. S6. A HDAC class III inhibitor, NAM (20mM), does not regulate RKIP mRNA levels in TNBC cells. MDA-MB-231, MDA-MB-436 and 1833 cells were treated for the indicated times with NAM (20 mM). RKIP mRNA levels were analyzed by qRT-PCR. Error bars represent SEM value from 3 independent experiments

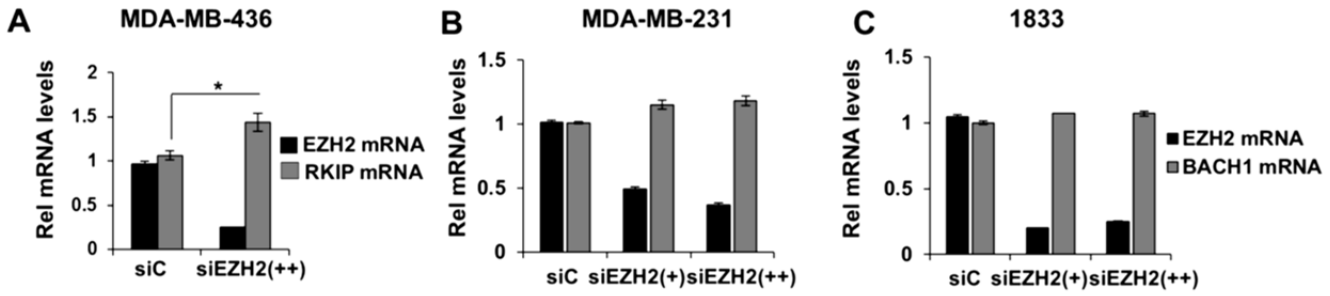

Fig. S7. EZH2 depletion increased RKIP levels but not regulate BACH1 mRNA levels. Transient depletion of EZH2 by siRNA (100 nM) for 48 hrs induced RKIP mRNA levels in MDA-MB-436 (**A**), while not regulated BACH1 mRNA levels in MDA-MB-231 (**B**) or 1833 cells (**C**). Relative mRNA for RKIP and EZH2 were analyzed by qRT-PCR.Error bars represent SEM value from 3 independent experiments. * indicates $p<0.05$ with Student's *t-test*.

2. Ultrasensitivity of BACH1 regulation by RKIP, through *let-7*

We started looking for ultrasensitivity because Angeli et al. showed in 2004 (5) that ultrasensitivity and positive feedback are necessary for bistability. The BACH1 to RKIP branch is most likely not ultrasensitive (apparently only one site is bound by BACH1 to repress RKIP). Therefore, the RKIP to BACH1 branch must be ultrasensitive for bistability to occur.

We start by studying *let-7* (*L*) regulation of BACH1 (*B*) transcript level as an isolated link (Fig. S8A). This can be modeled by the following system of Ordinary Differential Equations (ODEs):

$$\frac{dL}{dt} = a - L - cLB$$
$$\frac{dB}{dt} = S - B - cLB$$

where *a*=*let-7* synthesis rate; *c*=*let-7*+BACH1 binding rate; *S*=BACH1 synthesis rate.

At steady state we have:

$$L = \frac{a}{1+cB} \Rightarrow cLB = \frac{acB}{1+cB} \Rightarrow S = B\frac{1+cB+ac}{1+cB}$$

From here, we obtain a quadratic equation:

$$cB^2 + B(1+ac-cS) - S = 0$$

The only acceptable (positive) solution of the quadratic equation will be:

$$B = \frac{-(1+ac-cS) + \sqrt{(1+ac-cS)^2 + 4cS}}{2c}$$

The effect of the two parameters *S* and *c* on BACH1 response to *let-7* is shown in Figs. S8B and S8C. Overall, this analysis indicates that BACH1 mRNA response to *let-7* synthesis rate can become increasingly ultrasensitive as *c* or *S* increases.

RKIP regulates *let-7* expression indirectly via the Raf-1/MEK/Erk/Myc/Lin28 pathway (Fig. S8D). Overall, the dependence of *let-7* synthesis on RKIP could be modeled as a Hill function (Figs. S8E And S8F):

$$L = \frac{R^r}{m^r + R^r}$$

where *r* is the Hill coefficient and *m* is the threshold level for RKIP required for *let-7* activation.

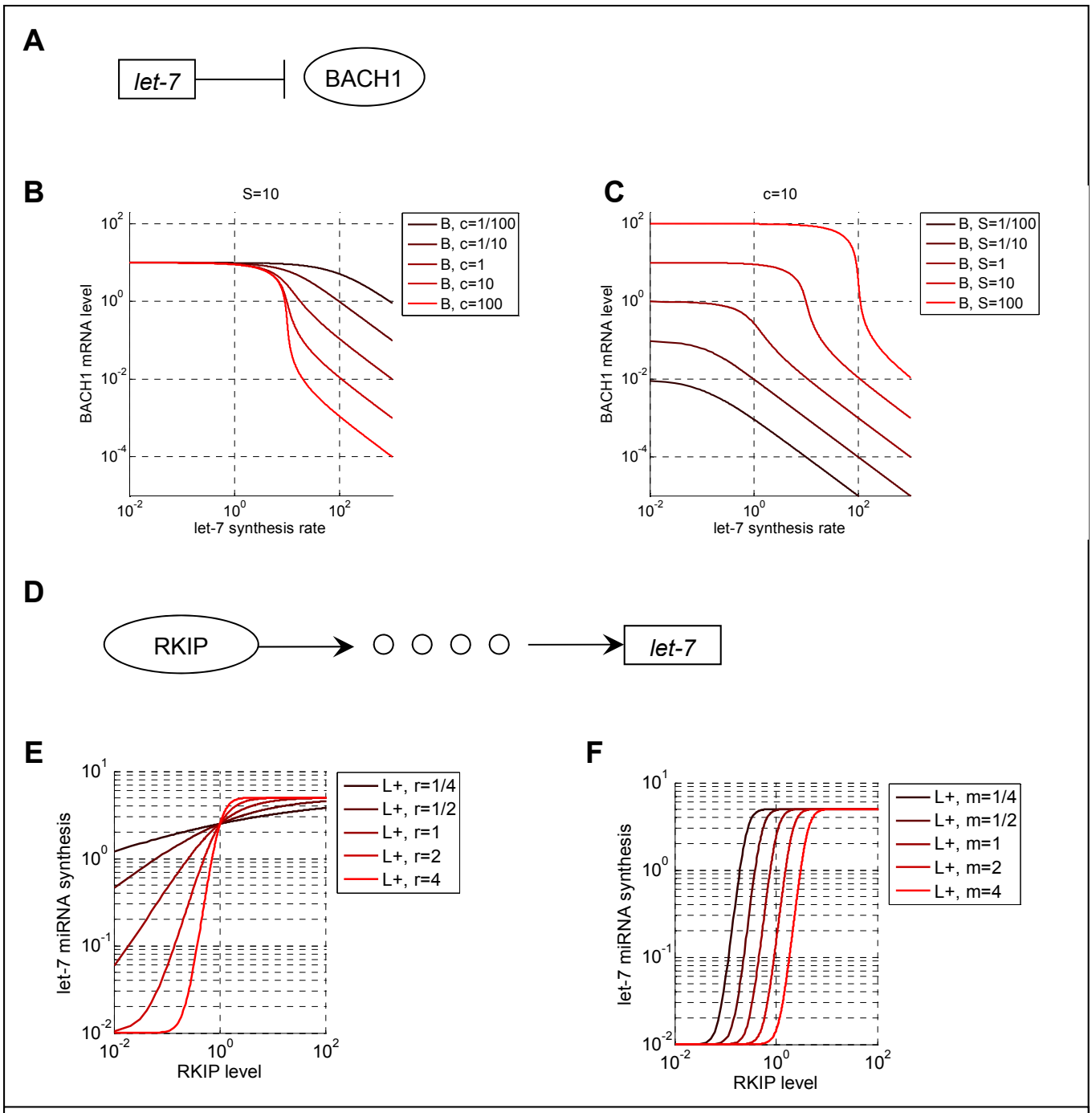

Figure S8. Ultrasensitivity along the RKIP-BACH1 regulatory branch. (A) Schematic illustration of BACH1 mRNA inhibition by *let-7*. (B) Response of BACH1 mRNA to the rate of *let-7* synthesis, for increasing rates of *let-7* binding to its target. (C) Response of BACH1 mRNA to increasing rates of *let-7* synthesis, for increasing rates of BACH1 mRNA synthesis. (D) Schematic illustration of indirect *let-7* microRNA inhibition by RKIP. (E) Response of *let-7* synthesis rate to RKIP, for increasing values of the Hill coefficient. (F) Response of *let-7* synthesis rate to RKIP, for increasing *let-7* sensitivity (threshold level of RKIP required for *let-7* induction).

Next, we join the RKIP to *let-7* and *let-7* to BACH1 pathways, to construct the full regulatory branch stretching from RKIP to BACH1, including BACH1's repression by *let-7* (Fig. S9A).

The ultrasensitivities of the two branches jointly result in ultrasensitive response of BACH1 mRNA to RKIP protein levels, as shown in Fig S9B, S9C, S9D and S9E.

Overall, this analysis indicates that the RKIP-BACH1 system satisfies the necessary conditions for bistability: it has an overall positive feedback loop involving a highly ultrasensitive branch. We investigate the complete RKIP-BACH1 feedback loop in the following section.

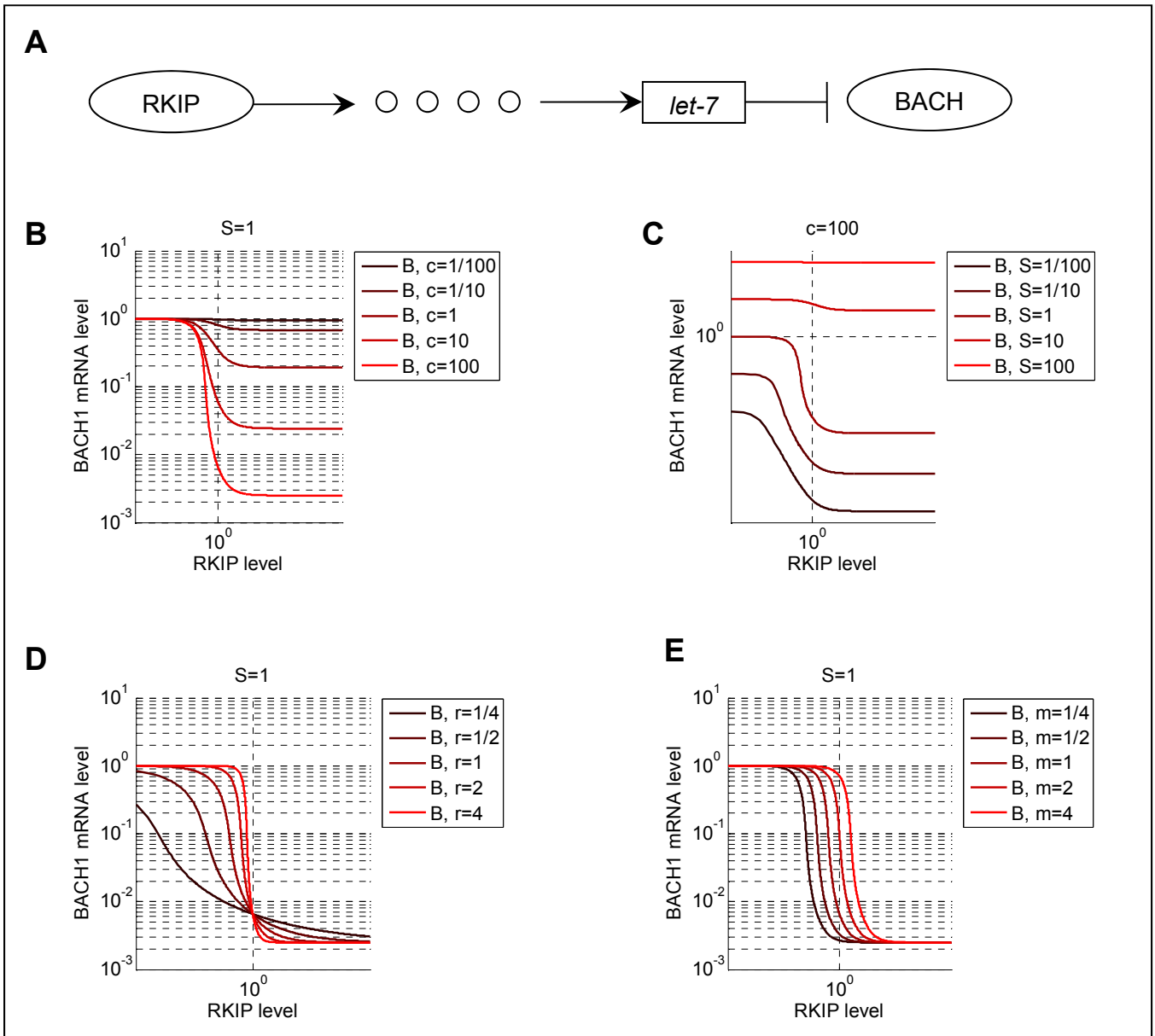

Figure S9. Ultrasensitivity in the full RKIP-BACH1 regulatory branch. (A) Schematic illustration of BACH1 inhibition by RKIP, through *let-7*. (B) Response of BACH1 mRNA level to RKIP, for increasing rates of *let-7* binding to its target. (C) Response of BACH1 mRNA level to RKIP, for increasing rates of BACH1 mRNA synthesis. (D) Response of BACH1 mRNA level to RKIP, for increasing values of the Hill coefficient. (E) Response of BACH1 mRNA level to RKIP, for increasing *let-7* sensitivity (threshold level of RKIP required for *let-7* induction).

3. The complete network: joining the BACH1- RKIP and RKIP-BACH1 arms

We established a system of ODEs to model the full RKIP-BACH1 system (see the Addendum). After rescaling the parameters, RKIP protein (R) regulation by BACH1 protein (not ultrasensitive) can be modeled as:

$$\frac{dR}{dt} = \frac{1}{1+B} - \rho R \qquad \text{OR} \qquad \frac{dR}{dt} = \frac{a_R}{1+B} - \rho R$$

Reactions between *let-7* miRNA (L) and BACH1 mRNA (B) assumed proportional with BACH1 protein:

$$\begin{aligned} \frac{dL}{dt} &= \frac{aR^r}{m^r + R^r} - L - cLB \\ \frac{dB}{dt} &= s + \frac{(S-s)K^b}{K^b + B^b} - B - cLB \end{aligned} \qquad \text{OR} \qquad \begin{aligned} \frac{dL}{dt} &= \frac{a_L R^r}{1+R^r} - L - cLB \\ \frac{dB}{dt} &= s + \frac{(S-s)K^b}{K^b + B^b} - B - cLB \end{aligned}$$

Assuming that the equation for L has fast dynamics, it equilibrates to steady state:

$$L = \frac{aR^r}{(m^r + R^r)(1+cB)}.$$

$$cLB = \frac{aR^r}{m^r + R^r} - L = \frac{aR^r}{m^r + R^r} - \frac{aR^r}{(m^r + R^r)(1+cB)} = \frac{aR^r}{m^r + R^r}\left[1 - \frac{1}{1+cB}\right] = \frac{cB}{1+cB}\frac{aR^r}{m^r + R^r}$$

The equation describing the dynamics of BACH1 becomes:

$$\frac{dB}{dt} = s + \frac{(S-s)K^b}{K^b + B^b} - B - \frac{aR^r}{m^r + R^r}\frac{cB}{1+cB}.$$

From here, we obtain the following system for BACH1 mRNA (B) and RKIP protein (R):

$$\begin{aligned} \frac{dB}{dt} &= s + \frac{(S-s)K^b}{K^b + B^b} - B\left[1 + \frac{c}{1+cB}\frac{aR^r}{m^r + R^r}\right] \\ \frac{dR}{dt} &= \frac{1}{1+B} - \rho R \end{aligned}$$

At equilibrium (steady state) the gain (e.g., transcription) and loss (e.g., degradation) are equal:

$$\underbrace{s + \frac{(S-s)K^b}{K^b + B^b}}_{gain} - \underbrace{B\left[1 + \frac{ac}{[m^r \rho^r (1+B)^r + 1](1+cB)}\right]}_{loss} = 0 \text{ since } R = \frac{1}{\rho(1+B)}.$$

4. Conditions for bistability

The BACH1 "gain" term $f(B)$ is a decreasing function of BACH1 (due to self-repression). If the BACH1 "loss" term were a monotone increasing function of BACH1, then the "loss" and "gain" terms would intersect in a single intersection point, and there could not be bistability.

We investigate the derivative to understand the trends of the BACH1 "loss" term. After some algebra, we obtain the derivative

$$f'(B) = 1 + \frac{ac}{[m^r \rho^r (1+B)^r + 1](1+cB)} - \frac{ac^2 B[m^r \rho^r (1+B)^r + 1] + acBm^r \rho^r r(1+B)^{r-1}(1+cB)}{[m^r \rho^r (1+B)^r + 1]^2 (1+cB)^2}$$

The BACH1 "loss" term at B=0 will be increasing because its slope $f'(0) = 1 + \frac{ac}{(m^r \rho^r + 1)} > 0$.

The "loss" term also tends asymptotically towards linear-increasing at high BACH1: $f'(\infty) = 1$. Considering that the BACH1 "gain" term $g(B)$ is monotone decreasing, bistability requires that the BACH1 "loss" term takes a "dip" somewhere between 0 and infinity, implying the existence of a peak and then a minimum, somewhere at intermediate BACH1 levels. This means that the derivative of the BACH1 "loss" term, $f'(B)$ must be negative over a range of intermediate BACH1 levels between two points B_1 and B_2 where $f'(B) = 0$. After some approximations ($1 + cB \approx cB$ for large B and $(1+B)^r \approx (1+rB)$ for small B) we find that the roots of $f'(B)$, B_1 and B_2 should approximately satisfy:

$$1 = ac \frac{m^r \rho^r (rcB_1^{\,2} - 1) - 1}{[m^r \rho^r (1 + rB_1) + 1]^2 (1 + cB_1)^2}$$

$$ar = [m^r \rho^r (1 + B_2)^r + 2](1 + B_2).$$

In addition to the existence of two roots for $f'(B)$, bistability requires that the BACH1 "gain" term intersects $g(B)$ the BACH1 "loss" term between the two extrema B_1 and B_2. For this, the following inequalities must be fulfilled:

$$g(B_1) < f(B_1)$$
$$g(B_2) > f(B_2).$$

Armed with these insights, we are able to delineate not only domains of bistability in the parameter space, but also domains of monostability where the equilibrium BACH1 levels are low (anti-metastatic cellular state) or high (pro-metastatic cellular state) relative to a threshold. Assuming that bistable regions separate anti-metastatic and pro-metastatic domains, a threshold can be selected between the two extrema B_1 and B_2 while the system is bistable, and then be preserved even after some parameter change makes the system monostable. This means that the threshold can change depending on parameter, which is not unreasonable because different cell lines may have different thresholds. Moreover, being pro- or anti-metastatic indicates only a tendency, not an actual metastatic phenotype.

5. Bistability is unlikely for parameter values corresponding to normal cells

We performed a literature search to identify reasonable parameter values in the RKIP-BACH1 system. We inferred some of these parameters by assuming that experimentally measured protein and mRNA levels correspond to equilibrium concentrations established by equal synthesis and degradation rates.

Protein and mRNA levels

R	RKIP protein	4.2 x10^6 molec./cell; mRNA: ~167 molec./cell (6). RKIP protein range: from 8x10^5 – 6x10^6 molecules/cell.
L	*let-7* microRNA	~2x10^3 molec./cell in *C. elegans*, BioNumbers and Ref. (7).
B	BACH1 mRNA	~30 copies/cell; protein: ~3 x10^3 molecules/cell (8).

Nominal parameters (concentration = number of molecules per cell, cell volume = 1)

$a_R = 5000/h$	max. rate of RKIP protein synthesis (transcr.=10/h × translation=648/h)
$\rho = 0.001 \div 0.004/h$	RKIP protein degradation (mRNA degr. rate = 0.04/h) (6)
$p = 100/h$	BACH1 protein synthesis rate per mRNA template (translation rate)
$s = 0.01 \div 1/h$	basal BACH1 mRNA expression
$S = 10 \div 1000/h$	max. rate of BACH1 mRNA synthesis (transcription)
$a_L = .05 \div 5 \times 10^3/h$	max. rate of *let-7* miRNA synthesis
$\mu = 0.5/h$	*let-7* microRNA and BACH1 mRNA degradation rate (BioNumbers)
$c = 10 \div 500$	*let-7* microRNA binding rate to BACH1 mRNA
$m = 10^2 \div 10^5$	RKIP protein threshold needed for *let-7* activation
$K_R = 100$	BACH1 protein threshold needed for RKIP repression
$K = 10 \div 10^3$	BACH1 protein threshold needed for BACH1 repression
$r = 2 \div 10$	Hill coefficient for *let-7*'s response to RKIP protein
$b = 1,2,3$	Hill coefficient for BACH1's response to BACH1 protein

We studied the effect of scanning the rescaled parameters around these nominal values (see the Appendix for the conversion of the original to the rescaled parameters) on rate-balance plots.

$\rho = 0.005$	RKIP protein degradation (drops 100-fold when destabilized)
$a = 1000$	maximum rate of *let-7* miRNA synthesis
$s = 0.02$	basal BACH1 mRNA expression
$S = 20$	maximum rate of BACH1 mRNA synthesis (transcription)
$c = 200$	*let-7* microRNA binding rate to BACH1 mRNA
$m = 2$	RKIP protein threshold needed for *let-7* activation
$K = 10$	BACH1 protein threshold needed for BACH1 repression
$r = 5$	Hill coefficient for *let-7*'s response to RKIP protein
$b = 3$	Hill coefficient for BACH1's response to BACH1 protein

The rate-balance plots in Fig. S10 show BACH1 gain (red) and BACH1 loss (blue) as functions of BACH1. Apparently, nominal parameters enforce an anti-metastatic state with low BACH1 equilibrium levels, located at the intersections of BACH1 gain (red) and BACH1 loss (blue) curves.

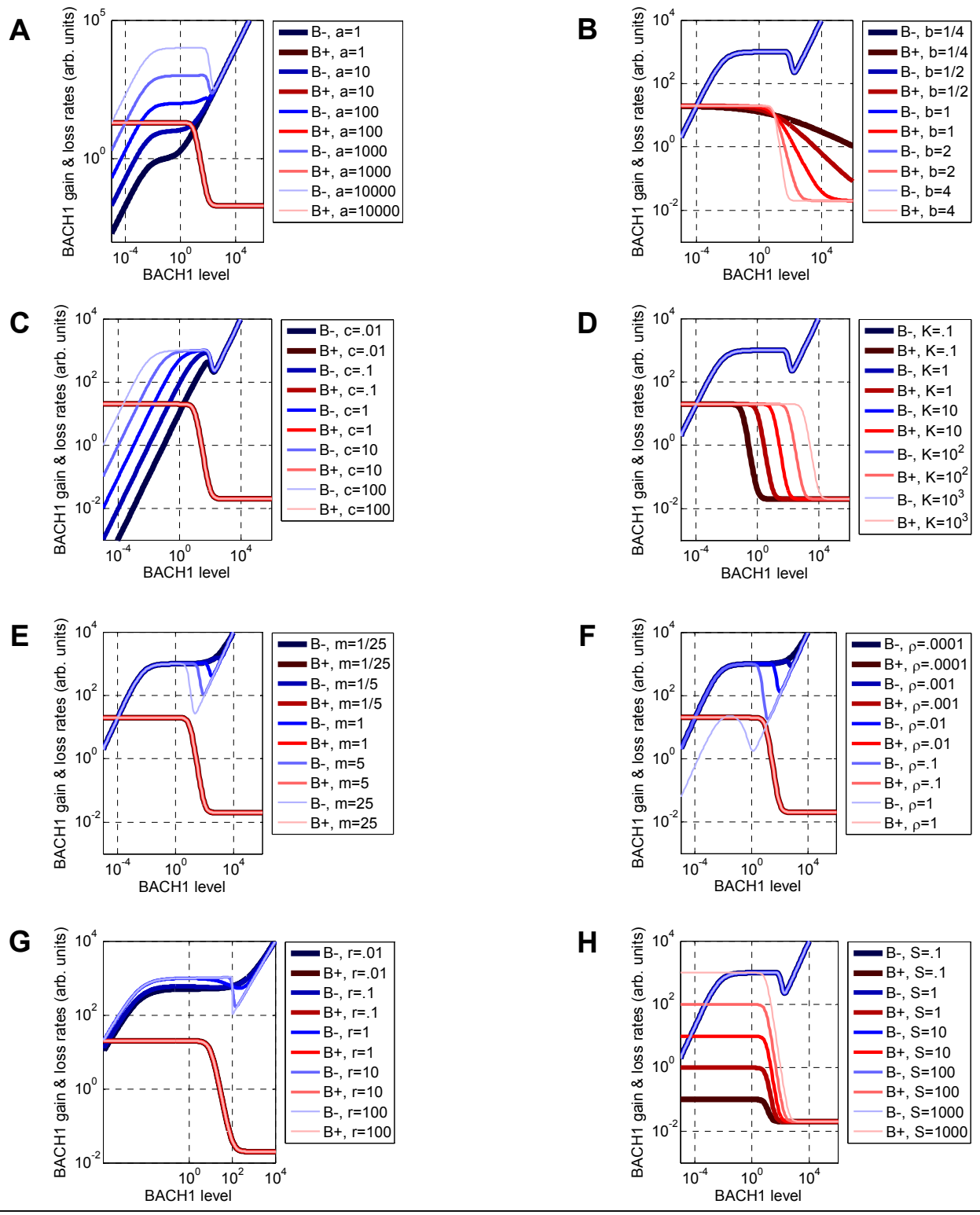

Figure S10. The effect of parameter changes around their nominal values on BACH1. (A) Increasing *let-7* synthesis rate causes a decrease in BACH1 levels. (B) Increasing BACH1's autoregulation slope has negligible effect on BACH1. (C) Increasing *let-7* binding rate to BACH1 mRNA causes a decrease in BACH1 levels. (D) Increasing BACH1's autoregulation threshold has negligible effect on BACH1. (E) Increasing the RKIP threshold for *let-7* activation may cause bistability. (F) Increasing RKIP degradation rate causes bistability. (G) Increasing the slope of *let-7* response to RKIP has negligible effect on BACH1. (H) Increasing maximum BACH1 synthesis rate causes an increase in BACH1 towards metastatic levels without bistability.

The plots in Fig. S10 indicate that certain parameter changes can bring the system closer to bistability and the pro-metastatic high BACH1 state. In particular, decreasing a (*let-7* synthesis rate) causes BACH1 increase towards pro-metastatic levels in a monostable-monostable (M-M) manner (Fig. S10A); decreasing c (*let-7* binding rate to BACH1) causes BACH1 increase (M-M transition, Fig. S10C); increasing ρ (RKIP degradation, Fig. S10F) causes BACH1 increase (B-M transition); and increasing S (maximum BACH1 synthesis) elevates equilibrium BACH1 levels (M-M transition, Fig. S10H).

Fig. S10 shows the effect of individual parameter changes. Multiple parameters could change at once and affect BACH1 steady state in a more complex manner. Yet, visualizing these transitions is difficult in the multidimensional parameter space. To gain better understanding of where an anti-metastatic cell resides relative to pro-metastatic, high BACH1 parameter sets, in Fig. S11 we plotted a cell (nominal parameters; red circle) in 2-dimensional parameter space, relative to anti-metastatic (white), pro-metastatic (black) and bistable (gray) domains. These figures, in concordance with the BACH1 gain and loss curves, pinpoint parameter changes that move the system into the pro-metastatic, high BACH1 state. Such perturbations could originate from mutations, stochastic fluctuations or the tissue microenvironment. For example, destabilizing RKIP will push the cells into a pro-metastatic state. Likewise, increasing BACH1 transcription *and* BACH1 self-threshold will result in bistability. Below we study the movement of this red circle (normal cell) after a 100-fold decrease in RKIP stability (Figs. S12, S13), and after a 35-fold increase in BACH1 transcription (Fig. S14).

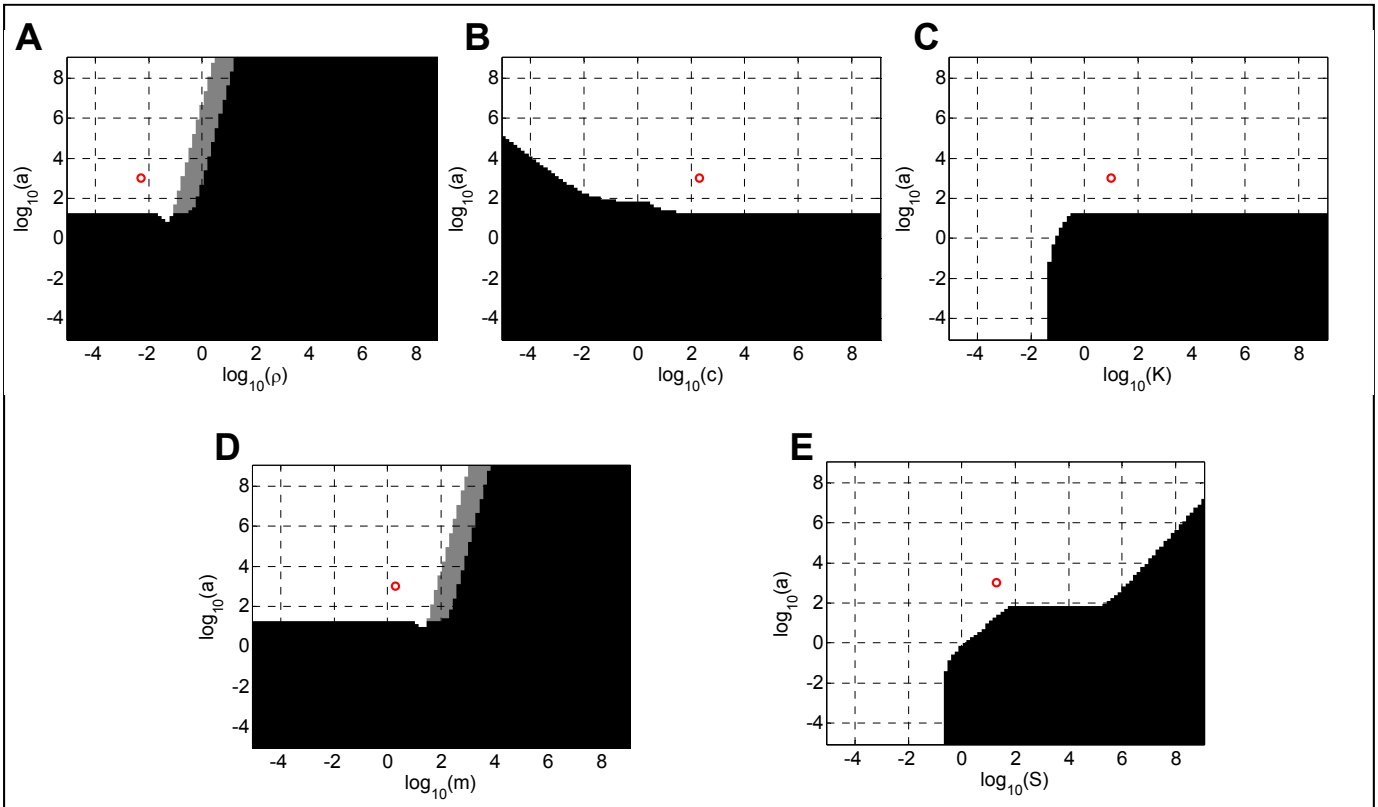

Figure S11. Normal cells (red) reside in monostable anti-metastatic (white) domains, away from bistability (gray) and pro-metastatic monostability (black). (A) The location of a normal cell in the (a,ρ) parameter space. (B) A normal cell in the (a,c) parameter space. (C) A normal cell in the (a,K) parameter space. (D) A normal cell in the (a,m) parameter space. (E) A normal cell in the (a,S) parameter space.

6. Towards metastasis, by destabilizing RKIP or increasing BACH1 transcription

To understand how a persistent fluctuation (which could be stochastic, environmental or genetic) alters RKIP-BACH1 dynamics, we re-plotted the cell in 2-dimensional parameter space as in Fig. S11 after increasing the RKIP degradation rate ρ 100-fold (Fig. S11, S12) or increasing BACH1 transcription 35-fold. The plots in Fig. S11 indicate that RKIP destabilization has two important effects on system dynamics. First, high RKIP instability enlarges the domains of bistability and reshapes the pro-metastatic and anti-metastatic domains. Second, the cell moves into the bistable domain (and into the pro-metastatic domain if RKIP stability is further compromised).

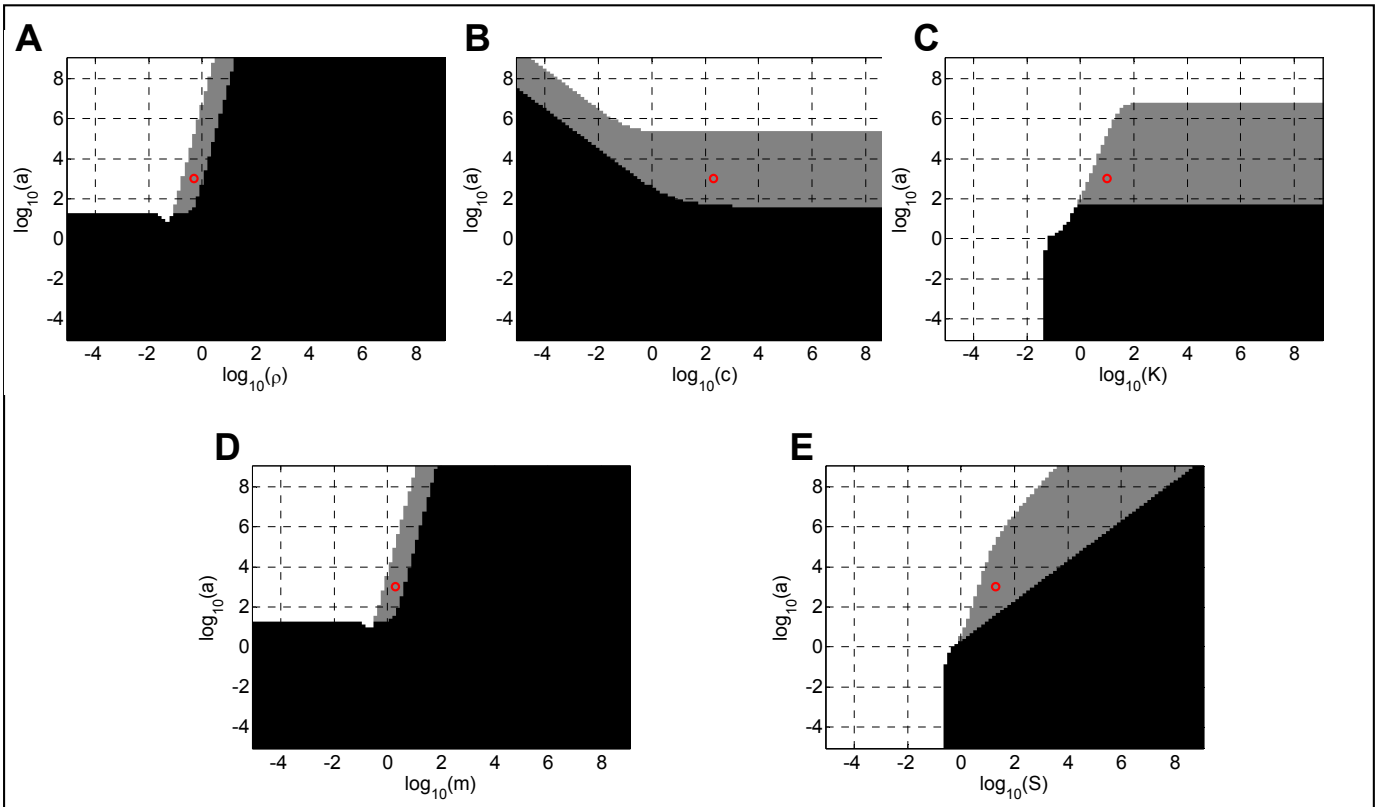

Figure S12. Cells with destabilized RKIP (red) reside in bistable (gray) domains, close to pro-metastatic monostability (black). (A) The location of a cell with unstable RKIP in the (a,ρ) parameter space. (B) The same cell in the (a,c) parameter space. (C) The same cell in the (a,K) parameter space. (D) The same cell in the (a,m) parameter space. (E) The same cell in the (a,S) parameter space.

While we obtained these shifts in the cell's position relative to the bistable domains by lowering RKIP stability, other parameter changes can have the same effect. For example, decreasing a (*let-7* synthesis rate), or c (*let-7* binding rate to BACH1), or increasing S (maximum BACH1 transcription rate) will also move the cell close to the borderline of the pro-metastatic domain.

Next, to study how further parameter changes affect the system once it becomes bistable, we studied the effect of parameter scans on rate-balance plots, while keeping RKIP levels 100-fold lower than normal (Fig. S13). We also studied the effect of parameter scans while keeping BACH1 transcription 35-fold higher and the BACH1 auto-threshold 10-fold higher (Fig. S14).

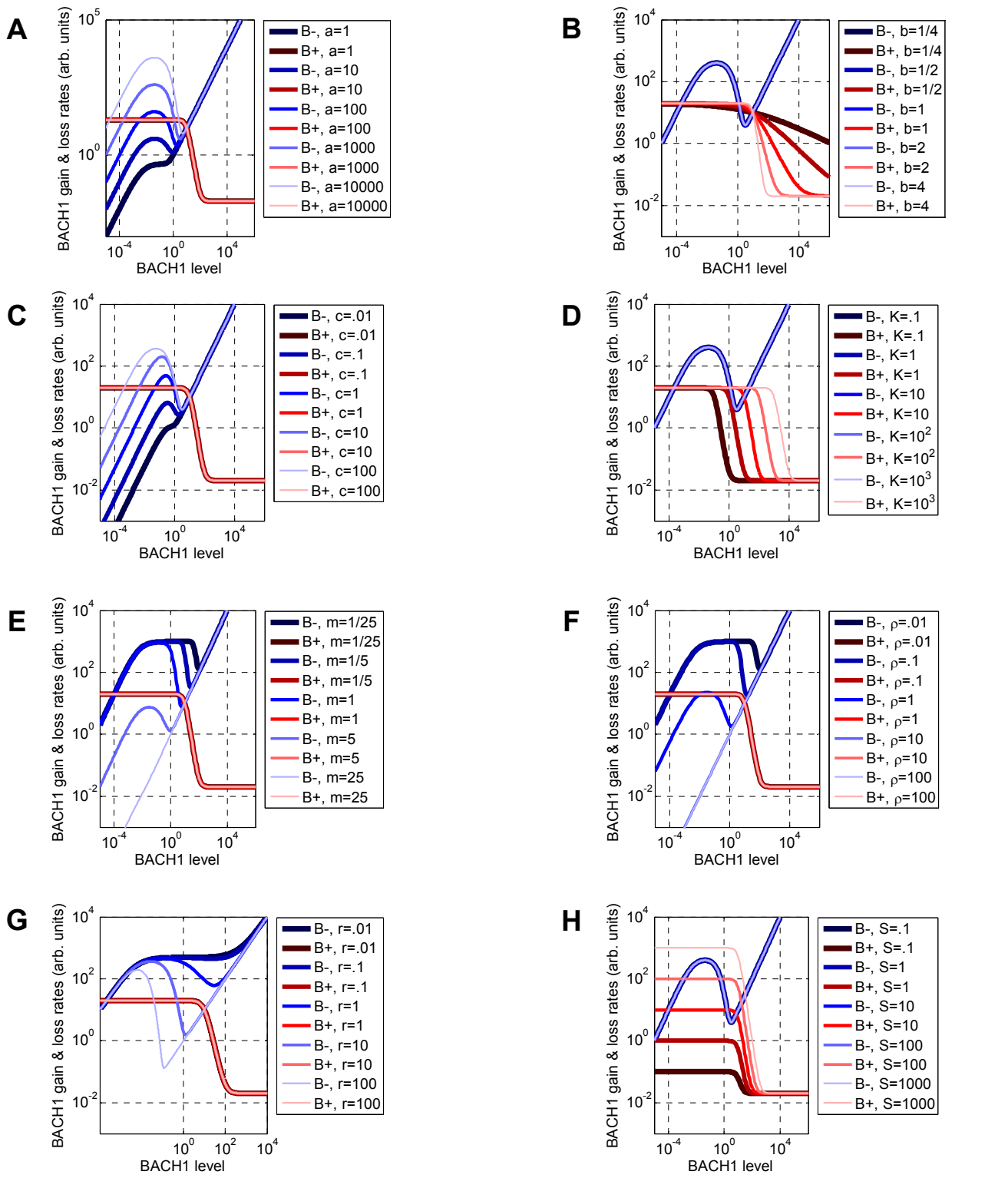

Figure S13. The effect of parameter changes on BACH1 when RKIP is unstable. (A) The effect of increasing *let-7* synthesis rate. (B) The effect of increasing BACH1's autoregulation slope (sensitivity) has negligible effect on BACH1. (C) The effect of increasing *let-7* binding rate to BACH1 mRNA. (D) The effect of increasing BACH1's autoregulation threshold (lowering its repressibility). (E) The effect of increasing the RKIP threshold for *let-7* activation. (F) The effect of increasing RKIP degradation rate. (G) The effect of increasing the slope of *let-7* response to RKIP. (H) The effect of increasing maximum BACH1 synthesis rate.

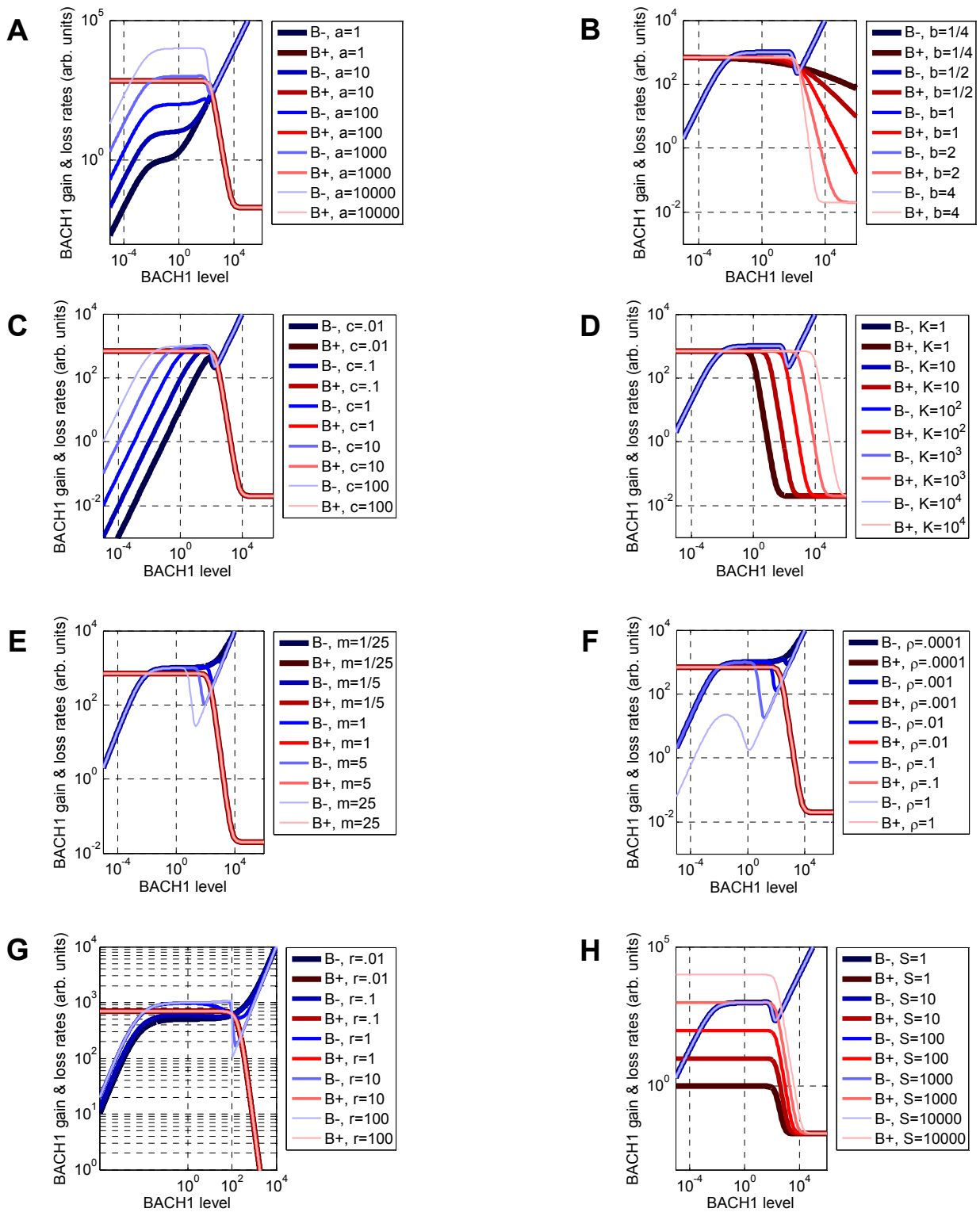

Figure S14. The effect of parameter changes at high BACH1 transcription. (A) The effect of increasing *let-7* synthesis rate. (B) The effect of increasing BACH1's autoregulation slope (sensitivity) has negligible effect on BACH1. (C) The effect of increasing *let-7* binding rate to BACH1 mRNA. (D) The effect of increasing BACH1's autoregulation threshold (lowering its repressibility). (E) The effect of increasing the RKIP threshold for *let-7* activation. (F) The effect of increasing RKIP degradation rate. (G) The effect of increasing the slope of *let-7* response to RKIP. (H) The effect of increasing maximum BACH1 synthesis rate.

7. Further insights from nullcline analysis

We determine the nullclines for the following system of two ODEs, to gain insight into the movement in phase space and the stability of steady states.

$$\frac{dB}{dt} = f(B,R) = s + \frac{(S-s)K^b}{K^b + B^b} - B\left[1 + \frac{aR^r}{m^r + R^r}\frac{c}{1+cB}\right]$$

$$\frac{dR}{dt} = g(B,R) = \frac{1}{1+B} - \rho R$$

Nullclines are curves obtained by setting each equation to 0, one by one.

$\frac{1}{1+B} - \rho R = 0 \Rightarrow R = \frac{1}{\rho(1+B)}$ or $B = \frac{1-\rho R}{\rho R}$ is the *R*-nullcline.

$$s + \frac{(S-s)K^b}{K^b + B^b} = B\left[1 + \frac{aR^r}{m^r + R^r}\frac{c}{1+cB}\right]$$

$$\frac{s(1+cB)}{acB} + \frac{(S-s)K^b(1+cB)}{acB(K^b + B^b)} - \frac{1+cB}{ac} = \frac{R^r}{m^r + R^r}$$

$$R^r\left\{1 - \left[\frac{s(1+cB)}{acB} + \frac{(S-s)K^b(1+cB)}{acB(K^b + B^b)} - \frac{1+cB}{ac}\right]\right\} = m^r\left[\frac{s(1+cB)}{acB} + \frac{(S-s)K^b(1+cB)}{acB(K^b + B^b)} - \frac{1+cB}{ac}\right]$$

$$R = m\left\{\frac{\frac{s(1+cB)}{acB} + \frac{(S-s)K^b(1+cB)}{acB(K^b + B^b)} - \frac{1+cB}{ac}}{1 - \left[\frac{s(1+cB)}{acB} + \frac{(S-s)K^b(1+cB)}{acB(K^b + B^b)} - \frac{1+cB}{ac}\right]}\right\}^{\frac{1}{r}}$$ is the *B*-nullcline.

The Jacobian matrix is given by:

$$\begin{bmatrix} \frac{\partial f}{\partial B} & \frac{\partial f}{\partial R} \\ \frac{\partial g}{\partial B} & \frac{\partial g}{\partial R} \end{bmatrix} = \begin{bmatrix} -\frac{b(S-s)K^b B^{b-1}}{(K^b + B^b)^2} - 1 - \frac{aR^r}{m^r + R^r}\frac{c}{(1+cB)^2} & -\left(\frac{acB}{1+cB}\right)\frac{rm^r R^{(r-1)}}{(m^r + R^r)^2} \\ -\frac{1}{(1+B)^2} & -\rho \end{bmatrix}$$

The largest eigenvalue of the Jacobian matrix at each steady state can estimate the stability of that state. Stable steady states have negative maximum eigenvalues, while unstable steady states have positive ones. This is illustrated in Fig. S15, where the system goes from monostable to bistable and then to monostable again as ρ increases from 0.1 (Fig. S15A) to 0.5 (Fig. S15B) and then 2 (Fig. S15C).

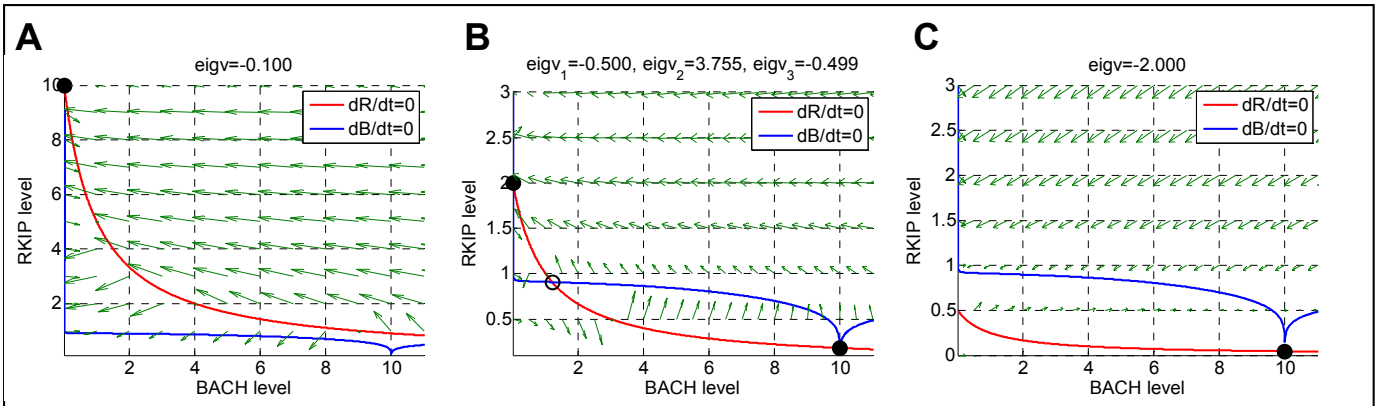

Figure S15. RKIP-nullcline (red), BACH1-nullcline (blue), and maximum eigenvalues as the system goes from monostable anti-metastatic to bistable and then to monostable pro-metastatic. (A) Monostable anti-metastatic condition for ρ=0.1. (B) Bistable condition for ρ=0.5. The open circle is an unstable steady state (it has a positive maximum eigenvalue). (C) Monostable pro-metastatic condition for ρ=2. The maximum eigenvalue for each BACH1 steady state is indicated above each plot.

Next, we studied how BACH1 negative autoregulation affects the stability of steady states. As indicated in Fig. S16 by the maximum eigenvalues of the third steady state, BACH1 autoregulation seems to stabilize the pro-metastatic state. This is probably true because direct BACH1 autoregulation counteracts BACH1 fluctuations. However, the overall stability of the pro-metastatic state may depend non-trivially on the other parameters in the system, meaning that no general statements can be made about the role of parameter *b* and the stability of the high BACH1 state.

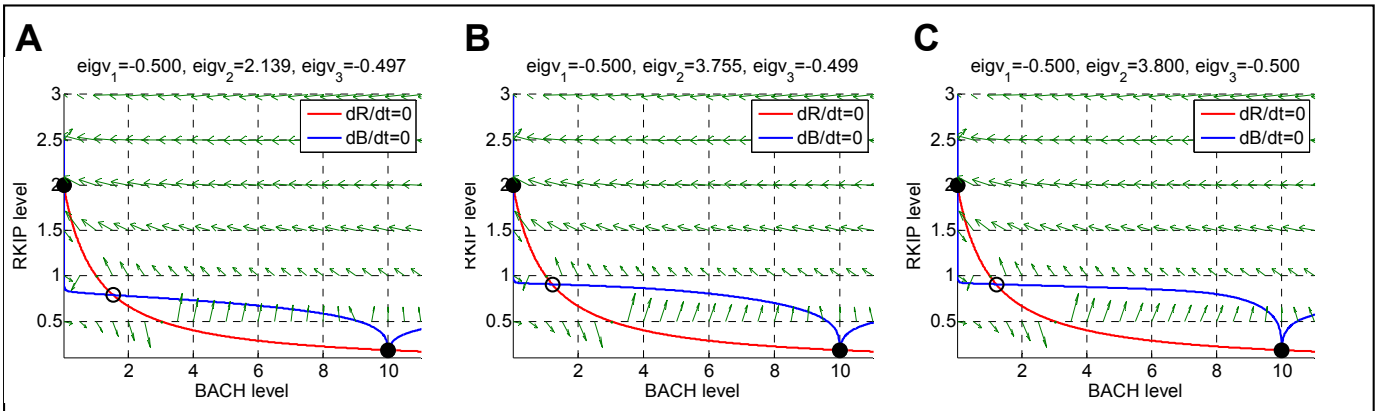

Figure S16. Nullclines and maximum eigenvalues for the bistable system as the parameter *b* is altered. (A) Monostable anti-metastatic condition for b=0.1. (B) Bistable condition for b=0.5. (C) Monostable pro-metastatic condition for b=10. The maximum eigenvalue for each BACH1 steady state is indicated above each plot.

8. Response of the RKIP-BACH1 network to random fluctuations

In living organisms, cells can be exposed to fluctuations arising from stochastic, environmental, and genetic factors. These fluctuations originate from random chemical reaction events, the position of a particular cell inside the tumor, or its genetic background, altering the parameters of the system. Although our lack of knowledge of appropriate parameters precludes truly stochastic simulations, we nevertheless decided to investigate the effect of fluctuations on the system.

Specifically, we studied the response of the RKIP-BACH1 system's steady state to random changes in 4 parameters: ρ (RKIP degradation rate), K (BACH1 dissociation constant from DNA), S (maximum BACH1 transcription rate), and a (maximum *let-7* synthesis rate). We picked a random number repeatedly from a lognormal distribution of mean = 1 and variance = 0.5, and multiplied it with the nominal value of the parameter. We solved the full system of three ODEs with random initial values over a sufficiently long time that it approached its steady state. The endpoint of each such simulation was considered to represent a single cell. We considered the histograms of these BACH1 steady states as rough approximation of BACH1 distributions in cancer cell populations.

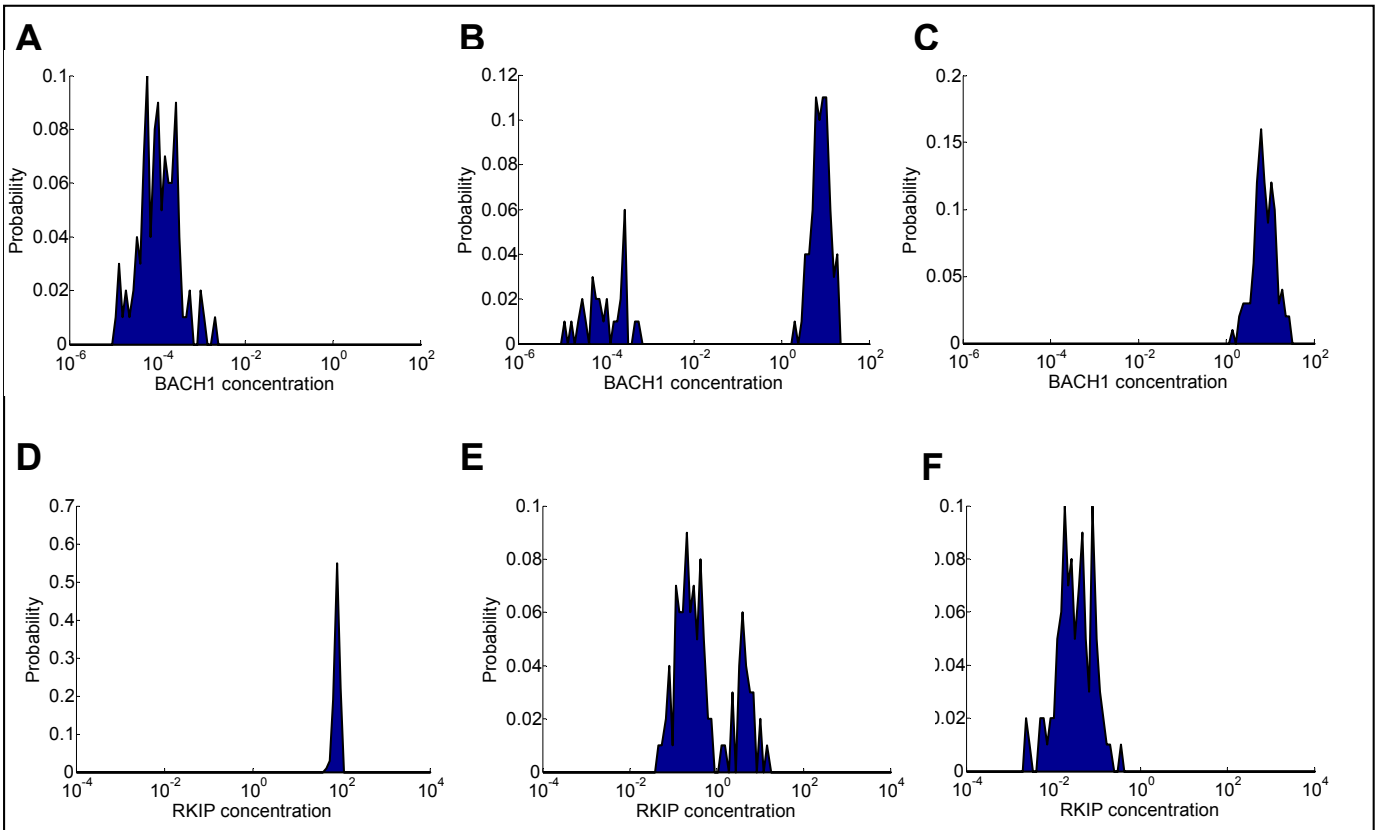

Figure S17. Response of BACH1 and RKIP levels to random fluctuations in 4 parameters. (A, D) Monostable anti-metastatic condition, for an average ρ=0.005. (B, E) Bistable condition for an average ρ=0.5. (C, F) Monostable pro-metastatic condition for an average ρ=5. The values of ρ, K, S, and a were repeatedly picked from lognormal distributions $\rho \times L(\rho+0.5,1)$, $K \times L(K+0.5,1)$, $S \times L(S+0.5,1)$, $a \times L(a+0.5,1)$.

9. The effect of BACH1 shRNA

We modified the system of ODEs to incorporate the effect of BACH1 shRNA by introducing term α equivalent to basal *let-7* miRNA (L) expression, considering that these molecules should have very similar effects (bind BACH1 mRNA and cause its degradation):

$$\frac{dL}{dt} = \alpha + \frac{aR^r}{m^r + R^r} - L - cLB \,.$$

Following the same strategy as for the original equations, we obtain at steady state:

$$L = \frac{1}{1+cB}\left[\alpha + \frac{aR^r}{m^r + R^r}\right], \text{ and } cLB = \alpha + \frac{aR^r}{m^r + R^r} - L = \frac{cB}{1+cB}\left[\alpha + \frac{aR^r}{m^r + R^r}\right].$$

The equation describing the dynamics of BACH1 mRNA (B) becomes:

$$\frac{dB}{dt} = s + \frac{(S-s)K^b}{K^b + B^b} - B - \frac{cB}{1+cB}\left[\alpha + \frac{aR^r}{m^r + R^r}\right].$$

At equilibrium (steady state) the gain (e.g., transcription) and loss (e.g., degradation) are equal:

$$\underbrace{s + \frac{(S-s)K^b}{K^b + B^b}}_{gain} - \underbrace{B\left[1 + \frac{c}{1+cB}\left(\alpha + \frac{a}{m^r \rho^r (1+B)^r + 1}\right)\right]}_{loss} = 0 \,.$$

Figs. S18 and S19 illustrate the effect of shBACH1 when applied in the bistable as well as the monostable pro-metastatic domain. In Fig. S18 the bistable and monostable pro-metastatic state were reached by lowering RKIP stability. By contrast, in Fig. S19 the bistable and monostable pro-metastatic state were reached by increasing BACH1 transcription and self-threshold.

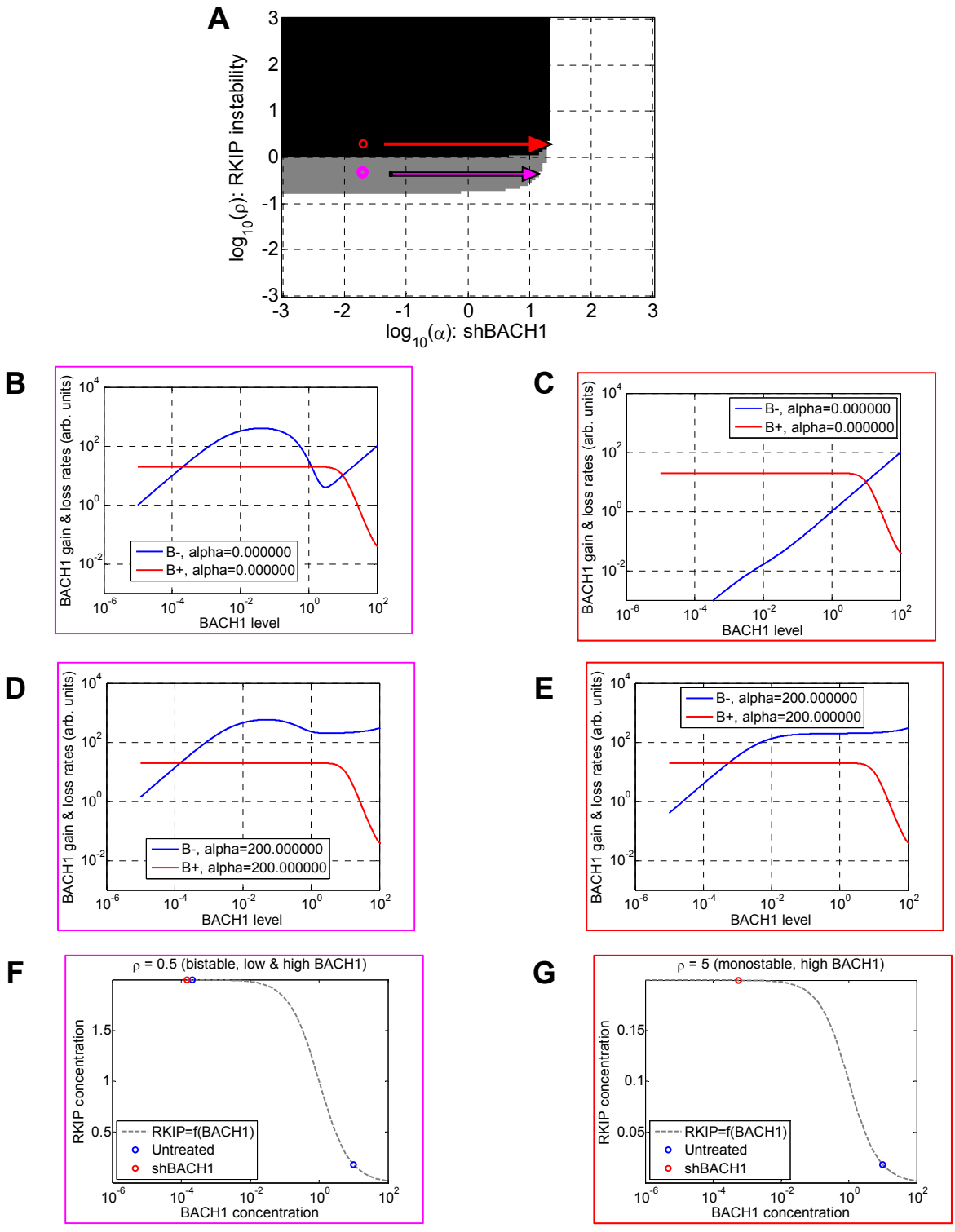

Figure S18. The effect of shBACH1 on a bistable or monostable pro-metastatic cell population. (A) Phenotype map for a cell in the pro-metastatic state, ρ=5. The red arrow indicates the effect of shBACH1 treatment. (B,D) Rate-balance plots indicating the effect of shBACH1 in the bistable (mixed) state, ρ=0.5. (C,E) Rate-balance plots indicating the effect of increasing shBACH1 expression in the monostable pro-metastatic state, ρ=5. (F) RKIP levels corresponding to the stable steady states in panels (B) and (D). (G) RKIP levels corresponding to the stable steady states in panels (C) and (E).

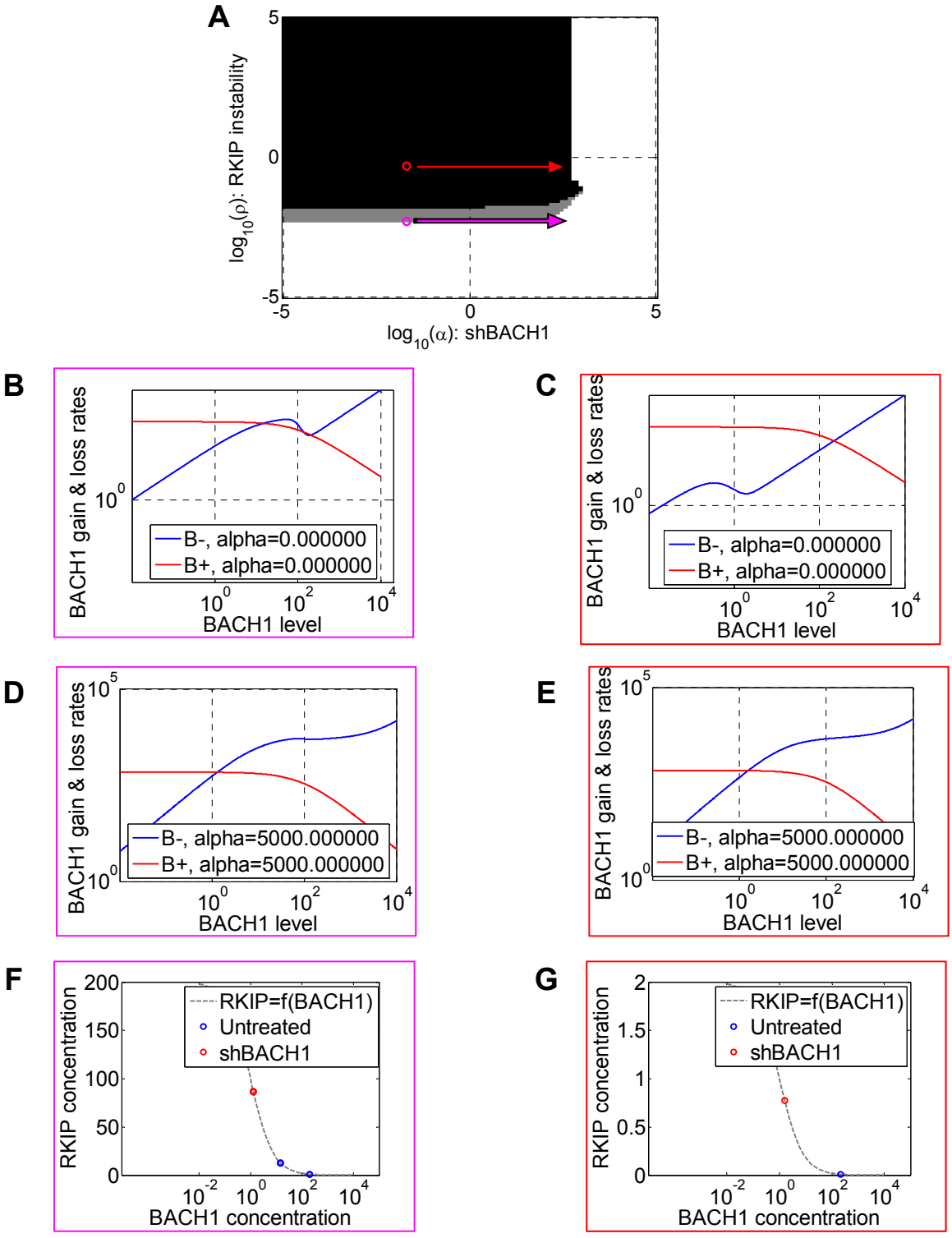

Figure S19. The effect of shBACH1 on cells with high BACH1 transcription. (A) Phenotype map for a cell in the pro-metastatic state, ρ=0.5. Red arrow: effect of shBACH1 treatment. (B,D) Rate-balance plots indicating the effect of shBACH1 in the bistable (mixed) state, ρ=0.005. (C,E) Rate-balance plots indicating the effect of increasing shBACH1 expression in the monostable pro-metastatic state, ρ=0.5. (F) RKIP levels corresponding to stable steady states in panels (B) and (D). (G) RKIP levels corresponding to stable steady states in panels (C) and (E). Other parameters: $a = 1000$; $s = 0.02$; $S = 700$; $c = .1$ $m = 2$; $K = 100$; $r = 5$; $b = 1$; $\alpha = 5000$.

10. Addendum: Rescaling the RKIP-BACH1 system to non-dimensional variables

$$\frac{dR}{dt} = \frac{a_R K_R}{K_R + pB} - \rho R$$
$$\frac{dL}{dt} = \frac{a_L R^r}{m^r + R^r} - \mu L - cLB$$
$$\frac{dB}{dt} = s + \frac{(S-s)K^b}{K^b + p^b B^b} - \mu B - cLB$$

#1: We first make the replacement: $t \mapsto Tt^*$. We have: $t^* = t/T$; $\frac{df}{dt} = \frac{df}{dt^*}\frac{dt^*}{dt} = \frac{1}{T}\frac{df}{dt^*}$.

$$\frac{dR}{dt^*} = \frac{a_R T K_R}{K_R + pB} - \rho TR$$
$$\frac{dL}{dt^*} = \frac{a_L T R^r}{m^r + R^r} - \mu TL - cTLB$$
$$\frac{dB}{dt^*} = sT + \frac{(S-s)TK^b}{K^b + p^b B^b} - \mu TB - cTLB$$

If $T = 1/\mu = 2h \Rightarrow$ $\rho \mapsto \rho/\mu$; $a_R \mapsto a_R/\mu$; $a_L \mapsto a_L/\mu$; $S \mapsto S/\mu$; $s \mapsto s/\mu$; $c \mapsto c/\mu$.

$$\frac{dR}{dt^*} = \frac{a_R}{1 + pB/K_R} - \rho R$$
$$\frac{dL}{dt^*} = \frac{a_L R^r}{m^r + R^r} - L - cLB$$
$$\frac{dB}{dt^*} = s + \frac{(S-s)K^b}{K^b + p^b B^b} - B - cLB$$

#2: Next replacement: $R \mapsto qR^*$. We have: $R^* = R/q$.

$$\frac{dR^*}{dt^*} = \frac{a_R/q}{1 + B\frac{p}{K_R}} - \rho R^*$$
$$\frac{dL}{dt^*} = \frac{a_L(\frac{q}{m}R^*)^r}{1 + (\frac{q}{m}R^*)^r} - L - cLB$$
$$\frac{dB}{dt^*} = s + \frac{(S-s)}{1 + \left(\frac{p}{K}\right)^b B^b} - B - cLB$$

If $q = m = 100 \Rightarrow\ a_R \mapsto a_R / m$ OR If $q = a_R = 5000 \Rightarrow\ m \mapsto m / a_R$

$$\frac{dR^*}{dt^*} = \frac{a_R}{1 + B\frac{p}{K_R}} - \rho R^* \qquad \frac{dR^*}{dt^*} = \frac{1}{1 + B\frac{p}{K_R}} - \rho R^*$$

$$\frac{dL}{dt^*} = \frac{a_L R^{*r}}{1 + R^{*r}} - L - cLB \qquad \frac{dL}{dt^*} = \frac{a_L R^{*r}}{m^r + R^{*r}} - L - cLB$$

$$\frac{dB}{dt^*} = s + \frac{(S-s)}{1 + \left(\frac{p}{K}\right)^b B^b} - B - cLB \qquad \frac{dB}{dt^*} = s + \frac{(S-s)}{1 + \left(\frac{p}{K}\right)^b B^b} - B - cLB$$

#3: Next replacement: $B \mapsto \beta B^*$. We have: $B^* = B / \beta$.

$$\frac{dR^*}{dt^*} = \frac{a_R}{1 + \beta B^* \frac{p}{K_R}} - \rho R^* \qquad \frac{dR^*}{dt^*} = \frac{1}{1 + \beta B^* \frac{p}{K_R}} - \rho R^*$$

$$\frac{dL}{dt^*} = \frac{a_L R^{*r}}{1 + R^{*r}} - L - cL\beta B^* \qquad \frac{dL}{dt^*} = \frac{a_L R^{*r}}{m^r + R^{*r}} - L - cL\beta B^*$$

$$\frac{dB^*}{dt^*} = \frac{s}{\beta} + \frac{(S-s)/\beta}{1 + (\beta \frac{p}{K} B^*)^b} - B^* - cLB^* \qquad \frac{dB^*}{dt^*} = \frac{s}{\beta} + \frac{(S-s)/\beta}{1 + (\beta \frac{p}{K} B^*)^b} - B^* - cLB^*$$

If $\beta = \frac{K_R}{p} = 1 \Rightarrow\ s \mapsto s\frac{p}{K_R};\ S \mapsto S\frac{p}{K_R};\ K \mapsto K\frac{p}{K_R}$.

$$\frac{dR^*}{dt^*} = \frac{a_R}{1 + B^*} - \rho R^* \qquad \frac{dR^*}{dt^*} = \frac{1}{1 + B^*} - \rho R^*$$

$$\frac{dL}{dt^*} = \frac{a_L R^{*r}}{1 + R^{*r}} - L - c\frac{K_R}{p} LB^* \qquad \frac{dL}{dt^*} = \frac{a_L R^{*r}}{m^r + R^{*r}} - L - c\frac{K_R}{p} LB^*$$

$$\frac{dB^*}{dt^*} = s + \frac{(S-s)K^b}{K^b + (pB^*)^b} - B^* - cLB^* \qquad \frac{dB^*}{dt^*} = s + \frac{(S-s)K^b}{K^b + (pB^*)^b} - B^* - cLB^*$$

#4: Next replacement: $L \mapsto \lambda L^*$. We have: $L^* = L / \lambda$.

$$\frac{dR^*}{dt^*} = \frac{a_R}{1+B^*} - \rho R^* \qquad \frac{dR^*}{dt^*} = \frac{1}{1+B^*} - \rho R^*$$
$$\frac{dL^*}{dt^*} = \frac{R^{*r} a_L / \lambda}{1+R^{*r}} - L^* - c\frac{K_R}{p} L^* B^* \qquad \frac{dL^*}{dt^*} = \frac{R^{*r} a_L / \lambda}{m^r + R^{*r}} - L^* - c\frac{K_R}{p} L^* B^*$$
$$\frac{dB^*}{dt^*} = s + \frac{(S-s)}{1+(\frac{p}{K}B^*)^b} - B^* - c\lambda L^* B^* \qquad \frac{dB^*}{dt^*} = s + \frac{(S-s)}{1+(\frac{p}{K}B^*)^b} - B^* - c\lambda L^* B^*$$

If $\lambda = \frac{K_R}{p} = 1 \Rightarrow\ a_L \mapsto \frac{a_L}{\lambda} = a_L \frac{p}{K_R}$.

$$\frac{dR^*}{dt^*} = \frac{a_R}{1+B^*} - \rho R^* \qquad \frac{dR^*}{dt^*} = \frac{1}{1+B^*} - \rho R^*$$
$$\frac{dL^*}{dt^*} = \frac{R^{*r} a_L}{1+R^{*r}} - L^* - c\frac{K_R}{p} L^* B^* \quad . \qquad \frac{dL^*}{dt^*} = \frac{R^{*r} a_L}{m^r + R^{*r}} - L^* - c\frac{K_R}{p} L^* B^*$$
$$\frac{dB^*}{dt^*} = s + \frac{(S-s)}{1+(\frac{p}{K}B^*)^b} - B^* - c\frac{K_R}{p} L^* B^* \qquad \frac{dB^*}{dt^*} = s + \frac{(S-s)}{1+(\frac{p}{K}B^*)^b} - B^* - c\frac{K_R}{p} L^* B^*$$

Final parameter changes: $\frac{K}{p} = K^* \mapsto K$ and $c\frac{K_R}{p} = c^* \mapsto c$.

$$\frac{dR^*}{dt^*} = \frac{a_R}{1+B^*} - \rho R^* \qquad \frac{dR^*}{dt^*} = \frac{1}{1+B^*} - \rho R^*$$
$$\frac{dL^*}{dt^*} = \frac{R^{*r} a_L}{1+R^{*r}} - L^* - cL^* B^* \qquad \frac{dL^*}{dt^*} = \frac{R^{*r} a_L}{m^r + R^{*r}} - L^* - cL^* B^*$$
$$\frac{dB^*}{dt^*} = s + \frac{(S-s)K^b}{K^b + B^{*b}} - B^* - cL^* B^* \qquad \frac{dB^*}{dt^*} = s + \frac{(S-s)K^b}{K^b + B^{*b}} - B^* - cL^* B^*$$

Finally, we drop the * notation:

$$\frac{dR}{dt} = \frac{a_R}{1+B} - \rho R \qquad \frac{dR}{dt} = \frac{1}{1+B} - \rho R$$
$$\frac{dL}{dt} = \frac{a_L R^r}{1+R^r} - L - cLB \quad . \qquad \frac{dL}{dt} = \frac{a_L R^r}{m^r + R^r} - L - cLB$$
$$\frac{dB}{dt} = s + \frac{(S-s)K^b}{K^b + B^b} - B - cLB \qquad \frac{dB}{dt} = s + \frac{(S-s)K^b}{K^b + B^b} - B - cLB$$

R	RKIP protein	(4.2 x10^6 molec. per cell; mRNA: ~167 molec./cell, PM:21593866) $8x10^5 - 6x10^6$
L	*let-7* microRNA	(~2x10^3 molec./cell in *C. elegans*, BioNumbers website, PM:12672692)
B	BACH1 mRNA	(~30 copies per cell; protein: ~3 x10^3 molec./cell PM:22068332)

Parameters (concentration = number of molecules per cell, cell volume = 1):

$a_R = 5000/h$	max. rate of RKIP protein synthesis (transcr.=10/h × translation=648/h)
$\rho = 0.001 \div 0.004/h$	RKIP protein degradation (mRNA degr. rate = 0.04/h) [PMID:21593866]
$K_R = 100$	BACH1 protein threshold needed for RKIP repression
$p = 100/h$	BACH1 protein synthesis rate per BACH1 mRNA (transl. rate lower: shRNA)
$s = 0.01 \div 1/h$	basal BACH1 mRNA expression
$S = 10 \div 100/h$	max. rate of BACH1 mRNA synthesis (transcription)
$a_L = .05 \div 5 \times 10^3/h$	max. rate of *let-7* miRNA synthesis
$\mu = 0.5/h$	*let-7* microRNA and BACH1 mRNA degradation rate (BioNumbers)
$c = 10 \div 500$	*let-7* microRNA binding rate to BACH1 mRNA
$r = 2 \div 10$	Hill coefficient for *let-7*'s response to RKIP protein
$m = 10^2 \div 10^5$	RKIP protein threshold needed for *let-7* activation
$K = 10 \div 10^3$	BACH1 protein threshold needed for BACH1 repression
$b = 1,2,3$	Hill coefficient for BACH1's response to BACH1 protein

New $\mapsto$ old:

$\rho \mapsto \rho/\mu = 2\rho$; $\rho = 0.002 \div 0.008$

$a_L \mapsto a_L \frac{p}{\mu K_R} = 2a_L$; $a_L = 100 \div 10000$

$S \mapsto S \frac{p}{\mu K_R} = 2S$; $S = 20 \div 200$

$s \mapsto s \frac{p}{\mu K_R} = 2s$; $s = 0.02 \div 2$

$c \mapsto c \frac{K_R}{\mu p} = 2c$; $c = 20 \div 1000$

$K \mapsto \frac{K}{K_R} = \frac{K}{100}$ $K = 0.1 \div 10^4$

$a_R \mapsto a_R/(\mu m) = a_R/50 = 100$ OR $m \mapsto m/a_R = m/5000 = 0.02 \div 20$

$\rho = 0.005$	RKIP protein degradation (drops 100-fold when destabilized)
$a_L = 1000$	maximum rate of *let-7* miRNA synthesis
$c = 200$	*let-7* microRNA binding rate to BACH1 mRNA
$s = 0.02$	basal BACH1 mRNA expression
$S = 20$	maximum rate of BACH1 mRNA synthesis (transcription)
$K = 20$	BACH1 protein threshold needed for BACH1 repression
$r = 5$	Hill coefficient for *let-7*'s response to RKIP protein
$b = 1,2,3$	Hill coefficient for BACH1's response to BACH1 protein

11. Supplementary References

1. Lehmann BD*, et al.* (2011) Identification of human triple-negative breast cancer subtypes and preclinical models for selection of targeted therapies. *J Clin Invest* 121(7):2750-2767.
2. Cheadle C, Vawter MP, Freed WJ, & Becker KG (2003) Analysis of microarray data using Z score transformation. *J Mol Diagn* 5(2):73-81.
3. Bourgon R, Gentleman R, & Huber W (2010) Independent filtering increases detection power for high-throughput experiments. *Proc Natl Acad Sci U S A* 107(21):9546-9551.
4. Perou CM*, et al.* (2000) Molecular portraits of human breast tumours. *Nature* 406(6797):747-752.
5. Angeli D, Ferrell JE, Jr., & Sontag ED (2004) Detection of multistability, bifurcations, and hysteresis in a large class of biological positive-feedback systems. *Proc Natl Acad Sci U S A* 101(7):1822-1827.
6. Schwanhausser B*, et al.* (2011) Global quantification of mammalian gene expression control. *Nature* 473(7347):337-342.
7. Lim LP*, et al.* (2003) The microRNAs of Caenorhabditis elegans. *Genes Dev* 17(8):991-1008.
8. Beck M*, et al.* (2011) The quantitative proteome of a human cell line. *Mol Syst Biol* 7:549.